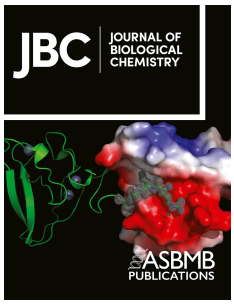

Cu, Fe and Zn isotope ratios in murine Alzheimer's disease models suggest specific signatures of amyloidogenesis and tauopathy

Nikolay Solovyev, Ahmed H. El-Khatib, Marta Costas-Rodríguez, Karima Schwab, Elizabeth Griffin, Andrea Raab, Bettina Platt, Franz Theuring, Jochen Vogl, Frank Vanhaecke

PII: S0021-9258(21)00060-0

DOI: https://doi.org/10.1016/j.jbc.2021.100292

Reference: JBC 100292

To appear in: *Journal of Biological Chemistry*

Received Date: 21 June 2020

Revised Date: 6 January 2021

Accepted Date: 11 January 2021

Please cite this article as: Solovyev N, El-Khatib AH, Costas-Rodríguez M, Schwab K, Griffin E, Raab A, Platt B, Theuring F, Vogl J, Vanhaecke F, Cu, Fe and Zn isotope ratios in murine Alzheimer's disease models suggest specific signatures of amyloidogenesis and tauopathy *Journal of Biological Chemistry* (2021), doi: https://doi.org/10.1016/j.jbc.2021.100292.

Cu, Fe and Zn isotope ratios in murine Alzheimer's disease models suggest specific signatures of amyloidogenesis and tauopathy

Nikolay Solovyev[1§¶], Ahmed H. El-Khatib[2,3§], Marta Costas-Rodríguez[1], Karima Schwab[4], Elizabeth Griffin[5], Andrea Raab[5,6], Bettina Platt[4], Franz Theuring[7], Jochen Vogl[2], Frank Vanhaecke[1*]

[1]Ghent University, Department of Chemistry, Atomic & Mass Spectrometry–A&MS research unit, Campus Sterre, Krijgslaan 281-S12, 9000 Ghent, Belgium
[2]BAM Bundesanstalt für Materialforschung und –prüfung, Richard-Willstätter-Str. 11, 12489 Berlin, Germany
[3]Department of Pharmaceutical Analytical Chemistry, Faculty of Pharmacy, African Union Authority St., Abbassia, Ain Shams University, Cairo, Egypt
[4]Institute of Medical Sciences, School of Medicine, Medical Sciences & Nutrition, Foresterhill, University of Aberdeen, Aberdeen, Scotland, AB25 2ZD, United Kingdom
[5]Trace Element Speciation Laboratory (TESLA), Department of Chemistry, University of Aberdeen, AB24 3UE, United Kingdom
[6]Institute of Chemistry, Environmental Analytical Chemistry, University of Graz, Universitätsplatz 1, 8010 Graz, Austria

[7]Charité – Universitätsmedizin Berlin, Institute of Pharmacology, Hessische Str. 3-4, 10115 Berlin, Germany
[§] Both authors contributed equally to this work.
[¶]Current address: Institute of Technology Sligo, Ash Lane, F91 YW50 Sligo, Ireland

*Corresponding author: Frank Vanhaecke: Ghent University, Department of Chemistry, Atomic & Mass Spectrometry–A&MS research unit, Campus Sterre, Krijgslaan 281-S12, 9000 Ghent, Belgium,
Tel: +32 9 264 48 48
E-mail: frank.vanhaecke@ugent.be

Running title: Cu, Fe and Zn isotopic profiles in brain & serum of AD mice

Keywords: Alzheimer's disease, tau, amyloid-beta, copper, iron, zinc, multi-collector inductively coupled plasma-mass spectrometry (ICP-MS), brain, serum, isotopic analysis, total element determination

Abstract

Alzheimer's disease (AD) is characterized by accumulation of tau and amyloid-beta in the brain, and recent evidence suggests a correlation between associated protein aggregates and trace elements, such as copper, iron and zinc. In AD, distorted brain redox homeostasis and complexation by amyloid-beta and hyperphosphorylated tau may alter the isotopic composition of essential mineral elements. Therefore, high-precision isotopic analysis may reveal changes in the homeostasis of these elements. We used inductively coupled plasma-mass spectrometry (ICP-MS)-based techniques to determine the total Cu, Fe and Zn contents in the brain, as well as their isotopic compositions in both mouse brain and serum. Results for male transgenic tau (Line 66, L66) and amyloid/presenilin (5xFAD) mice were compared to those for the corresponding age- and gender-matched wild-type control mice (WT). Our data show that L66 brains showed significantly higher Fe levels than the corresponding WT. Significantly less Cu, but more Zn was found in 5xFAD brains. We observed significantly lighter isotopic compositions of Fe (enrichment in the lighter isotopes) in the brain, and in serum of L66 mice compared to WT. For 5xFAD mice, Zn exhibited a trend towards a lighter isotopic composition in brain and a heavier isotopic composition in serum compared to WT. Neither mouse model yielded differences in the isotopic composition of Cu. Our findings indicate significant pathology-specific alterations of Fe and Zn brain homeostasis in mouse models of AD. The associated changes in isotopic composition may serve as a marker for proteinopathies underlying AD and other types of dementia.

Introduction

Alzheimer's disease (AD) is the most common cause of dementia, accounting for about two-thirds of the currently reported 50 million dementia cases worldwide. By 2050, about 152 million people are likely to be diagnosed with dementia. With a current cost of about a trillion US dollars a year (expected to double by 2030) and being a major cause of death, dementia is a growing global health concern that places a significant burden on societies and healthcare systems. Therefore, there is an urgent need to develop interventions and treatments to reverse or at least slow down the progression of AD (1-3). As early and specific diagnosis is essential for effective therapeutics, current research efforts also focus on the discovery of biomarkers (2,3) enabling disease detection during early stages (4).

The pathology of AD involves the misprocessing of the amyloid precursor protein (APP), which results in the accumulation and build-up of soluble and fibrillar amyloid-beta (Aβ) and other metabolites (5). Additionally, hyperphosphorylated tau, a microtubule-associated protein, leads to the formation of neurofibrillary tangles, composed of a truncated 100-amino acid fragment of tau (6), which can autonomously catalyse the conversion of normal soluble tau into tau fibrils and tau aggregates (7). Both, tau and Aβ aggregation contribute to AD pathology, but hypotheses differ as to which of these is the primary causative factor (8). Nevertheless, both are hallmarks of AD used for the ultimate post-mortem confirmation of AD (4).

Previous observations of hot spots of certain metals alongside tau/Aβ accumulation suggested that spatial or even mechanistic correlations exist between tau/Aβ and certain trace elements. Essential trace elements such as copper (Cu), iron (Fe) and zinc (Zn) have fundamental physiological roles in, *e.g.*, enzymatic reactions, oxygen transport and cellular signalling; their homeostasis is therefore crucial for proper functioning of the brain (9-11). Furthermore, elevated Cu, Fe and Zn levels were found in Aβ plaques in AD brain tissues (12-15), suggesting a direct or indirect involvement of trace metals in AD pathogenesis. Recent systematic reviews indicated weak associations between Cu, Fe and Zn and AD, with some studies reporting increased levels of these metals, while others are reporting decreased levels in the media investigated (predominantly blood and to a lesser extent cerebrospinal fluid (CSF), nails and hair) of AD patients (16,17). However, more mechanistic studies indicate several possible pathways relating Cu, Fe and Zn and AD pathology (18-20).

To date, both tau- and Aβ-based animal models are widely used in AD research. Several tau transgenic mouse models have been generated,

most of them based on overexpression of mutant tau (21,22), though it is important to note that these mutations are based on frontotemporal dementia (FTD) and not AD. Lines include for example the P301L mouse, which overexpresses the aforementioned mutation in the longest human tau isoform (htau40). Expression of P301L htau40 results in early deposition of tau tangles, gliosis, axonal degeneration and motor and behavioural deficits (23).

Line 66 (L66) mice express full-length human tau with the P301S mutation under the control of the Thy1-regulatory element (24). The P301S mutation has been previously associated with tau aggregation (25-27). L66 mice overexpress the longest human tau isoform (htau40) with 441 amino acid residues, under the control of the mouse *Thy1*-promoter. These mice show early onset high tau load in hippocampal and cortical neurons (24) and robust inflammation in both forebrain and hippocampal system (28) reminiscent of the behavioural variant of FTD with tau pathology. The L66 murine model has widely abundant tau pathology throughout the brain, with particularly high tau aggregation in neurons of the hippocampus and entorhinal cortex, eventually leading to neuronal loss (24). Behaviourally, these mice are characterized by abnormal gait pattern and dysfunction in motor coordination and motor learning as early as 4-5 weeks of age (24).

As for Aβ models, first attempts to generate AD-like pathology in mice by overexpressing APP were only partly successful, as mice tended to produce only low Aβ-associated pathology, and often failed to show behavioural impairments (29,30). Later, the familial AD model (5xFAD) was created by combining five mutations related to human APP and presenilin (an enzyme converting APP to Aβ (23), which are linked to autosomal dominant forms of familial AD (FAD) (31). The 5xFAD mice are double transgenic for APP and PSEN1 with a total of five AD-linked mutations: the Swedish (K670N/M671L), Florida (I716V), and London (V717I) mutations in the APP gene, as well as the M146L and L286V mutations in the PSEN1 gene. These mutations lead to accelerated Aβ plaque formation and deposition, and eventually to neuronal loss and working memory impairments (32,33). These mice are characterised by aggressive Aβ neuropathology and early behavioural deficits.

Both Line 66 and the 5XFAD models have been extensively characterized in terms of pathology and cognition (24,32,33) and were used in the current study for brain and serum analysis. We have used quadrupole-based and sector field inductively coupled plasma-mass spectrometry (ICP-MS) for quantification of the total element contents of Cu, Fe and Zn and multi-collector sector field inductively coupled plasma-mass spectrometry (MC-ICP-MS) for measuring their isotope ratios (expressed as delta (δ) values) and demonstrated the traceable and precise determination of the total element contents and isotope ratios of Cu, Fe and Zn.

Mutant tau expressing mice showed a lighter isotopic composition of Fe (enriched in the lighter isotopes) in the brain, and to a lower extent in blood serum, as well as higher Fe contents in the brain than matched wild-type (WT) mice. For the 5xFAD mice compared to controls, a trend towards a lighter Zn isotopic composition was observed in brain tissue and blood serum. The results of this study may provide a step forward concerning the potential use of the Cu, Fe and Zn isotopic information for diagnostic purposes and/or to achieve a more profound understanding of AD.

Results

Analytical methods applied in the different research facilities involved were evaluated and thereafter implemented for the traceable quantitative determination and for the accurate and precise isotopic analysis of Cu, Fe and Zn in brain tissue and blood serum of L66 and 5xFAD mice, as well as of their respective controls. The measurements undertaken and research facilities responsible are summarised in **Table 1**. Only SI-traceable data (here mass fractions) or data being traceable to the same internationally accepted source (accomplished *via* the use of delta values against internationally accepted isotopic reference materials) are metrologically comparable. The total elemental content quantification was validated between BAM and the University of

Aberdeen; isotope ratio measurements were validated between BAM and Ghent University.

TABLE 1 HERE

Given that diet is the major source of metal exposure and that mouse groups received different chows in the different housing facilities, the animals' chow was also analysed for its Cu, Fe and Zn isotopic compositions. L66 mice and their NMRI wild-type (NMRI-WT) controls (housed at Charité) received the same chow (V1534-3) for the first 10 months, but between 10 and 12 months (time of sacrifice) L66 received a different chow with higher protein content (V1124-3) because they developed a considerable tremor. Total contents of Cu, Fe and Zn in both types of chow were in line with the manufacturers' data. However, their δ^{65}Cu, δ^{66}Zn, δ^{67}Zn and δ^{68}Zn values were significantly different from each other (**Table S1**). Conversely, 5xFAD mice and their C57BL6/J wild-type (BL6-WT) controls received the same chow during the whole experimentation period; the total contents of Cu, Fe and Zn in this chow were in line with the manufacturers' data.

Total Cu, Fe and Zn levels in mouse brain

The total contents of Cu, Fe and Zn in mouse brain (per wet tissue weight) were determined by sector field and quadrupole-based inductively coupled plasma-mass spectrometry (SF-ICP-MS and Q-ICP-MS, respectively). Since the amount of serum collected was insufficient for accurate quantification, only isotopic analysis was conducted (see below).

Quantitative determination of the elements of interest in brain tissue indicated that L66 mice had higher contents of Fe than NMRI-WT (p<0.05, see **Figure 1** and supplementary **Table S2A**). Also for Cu and Zn, a higher content was observed in brain tissue of L66 mice, though the increase was not statistically significant (p=0.071 and p=0.455, respectively). *Post-hoc* analysis (the chow was analysed along with the mice brain and serum) of the metal contents in the diet of the animals did not suggest that differences in the metal contents of the diets were at the origin of these observations. Element quantification of 5xFAD brains (**Figure 1** and supplementary **Table S2B**), indicated significantly *lower* levels of Cu (p<0.05), but a higher content of Zn in brain tissue of 5xFAD mice compared to BL6-WT (p<0.01).

FIGURE 1 HERE

Isotopic signatures of Cu, Fe and Zn in mouse brain and blood serum

The isotopic compositions of Cu, Fe and Zn in brain tissue and blood serum were compared at group levels and the overall differences, expressed as δ-values, are presented in **Figures 2, 3** and **4** (detailed data in supplementary **Tables S3** & **S4)**. Additionally, individual δ-values all samples analysed are presented in the Supplementary data file.

FIGURES 2, 3 and 4 HERE

In the brain of L66 compared to NMRI-WT mice, δ^{56}Fe and δ^{57}Fe levels (p<0.001) indicated a significantly lighter Fe isotopic composition (enrichment in the lighter ^{54}Fe isotope) and this shift was partially confirmed for serum levels (p= 0.02 and 0.082 for δ^{56}Fe and δ^{57}Fe, respectively) – **Figure 3** (supplementary **Tables S3A** & **S4B** for brain and serum, respectively). The absolute shift between the L66 and NRMI was found to be Δ^{56}Fe = -0.16‰ and Δ^{57}Fe = -0.24‰ for brain. For serum, the values were as follows: Δ^{56}Fe = -0.30‰ and Δ^{57}Fe = -0.30‰. No significant differences in the Cu or Zn isotopic composition in brain or blood serum were observed between the L66 and NRMI-WT groups (**Figure 2** and **4**).

For the 5xFAD and BL6-WT groups (**Figure 3** and supplementary **Tables S3** & **S4**), no significant differences were established in terms of the Cu or Fe isotopic composition between mice, neither for brain nor serum. Interestingly, the isotopic composition Zn showed the trend of becoming lighter in the brain of 5xFAD mice (compared to BL6-WT), opposite effects were seen for the respective isotopic compositions in the serum. The δ^{67}Zn and δ^{68}Zn values (p=0.049 and p=0.034, respectively *vs.* p=0.081 for δ^{66}Zn) may indicate a lighter isotopic composition in the brain, while for serum, the δ^{67}Zn values (p=0.009) show an opposite tendency towards a heavier isotopic composition (depletion in the light ^{64}Zn isotope). However, for δ^{66}Zn and δ^{68}Zn, p were found to be 0.061 and 0.071, respectively. The absolute shift of isotopic composition for 5xFAD

vs. BL6-WT mice was as follows (brain/serum): Δ^{66}Zn = -0.13 / +0.09, Δ^{67}Zn = -0.26 / +0.17, Δ^{68}Zn -0.43 / +0.12‰.

Next, we systematically compared Cu, Fe and Zn isotopic compositions of brain and serum (**Figure 5**).

FIGURE 5 HERE

For NMRI-WT controls, we observed a positive correlation between brain and serum data for the three isotope ratios δ^{65}Cu, δ^{56}Fe and δ^{66}Zn (Pearson's R^2>0.35). In L66, δ^{65}Cu brain and serum values are likewise positively correlated (Pearson's R^2>0.45), but the overall δ^{65}Cu value in L66 is lower than in their WT controls (**Figures 5A**). In L66, and contrary to NMRI controls, the δ^{56}Fe values in brain and serum, respectively, did not correlate (**Figures 5C**, Pearson's R^2=0.04), while a similar positive correlation was seen for δ^{66}Zn (**Figures 5E**, Pearson's R^2>0.4). It should be noted though that only for δ^{65}Cu in L66 mice and δ^{66}Zn in both L66 and NMRI-WT statistical significance of the correlation was reached at p<0.05.

For both, 5xFAD and BL6-WT mice (**Figures 5**), we observed a positive and similar correlation, though weak, between brain and serum δ^{65}Cu values (**Figures 5B**, Pearson's R^2 between 0.2 and 0.3). In BL6-WT mice, the δ^{56}Fe values correlated fairly between brain and serum (**Figures 5D**, Pearson's R^2>0.2). However, in 5xFAD mice, this positive correlation for δ^{56}Fe is stronger (**Figures 5D**, Pearson's R^2>0.5, p<0.05), and in general this element is isotopically lighter in 5xFAD than in BL6 controls (compare the slopes of 2.50 *vs*. 0.75 for 5xFAD and BL6-WT mice, respectively, **Figures 5B**). Brain and serum δ^{66}Zn values (**Figures 5F**) correlated positively in 5xFAD mice (Pearson's R^2>0.4), but not in BL6-WT mice (Pearson's R^2<0.0001). In this case, only the correlation of δ^{56}Fe in 5xFAD mice reached statistical significance at p<0.05.

Discussion

High-precision isotopic analysis is an emerging approach for studying biochemical metal-related processes (34). For the lighter of any two isotopes, physicochemical processes proceed slightly faster (kinetic mass-dependent fractionation), while in chemical reactions, the heavier of any two isotopes has a slight preference for the strongest bonds (thermodynamic mass-dependent fractionation) at equilibrium (35). Biochemical processes may be accompanied by isotope fractionation, resulting in potential differences in the isotopic composition of a given metal between compartments. As biochemical processes are affected during disease processes, the isotopic composition of a metal in a given body compartment (*e.g.*, body fluid) may also be different in patients *vs.* controls. Current analytical techniques, such as MC-ICP-MS, offer the precision required to reveal and quantify such isotope fractionation (36). High-precision isotopic analysis is being explored as a diagnostic tool for diseases that can otherwise only be established at a later stage and/or *via* more invasive techniques, or for obtaining a more profound insight into biochemical processes involving the element of interest (37,38). So far, the isotopic composition of Cu was proven to be useful in the context of liver disease (39) and cancer (40,41), that of Fe as a robust marker of individual Fe status, also in cases in which the currently used markers are no longer reliable (42,43) and that of Zn in cancer (41,44,45). High-precision isotopic analysis has also been successfully applied in animal experiments to contribute to further insight into the factors governing the differences in isotopic composition (46-48).

Men and women with AD are known to exhibit different cognitive and psychiatric symptoms; women show a faster cognitive decline in AD and milder cognitive impairment (49). Such sex-dependent pattern is also reproduced in some *in vivo* models of AD (49,50). This seems to correspond also to the brain metal homeostasis (51). For instance, Maynard *et al.* demonstrated significantly decreased Fe, Cu and Zn levels in the brain of APP-overexpressing female mice, compared to males; but these sex-related differences were independent of APP/Aβ expression (52). Thus, to prevent such sex-related ambiguity, only male animals were investigated in the current study, which may be considered as a limitation since sex differences could not have been revealed.

In the current study, we observed δ^{56}Fe and δ^{57}Fe, values that significantly differed when comparing isotope ratios in brains of tau (L66), and NMRI-WT mice. The results indicate that the brain tissue of mice under tau-pathology is enriched in the lighter Fe and Zn isotopes. Also in L66 serum, Fe was found to be isotopically lighter compared to the WT. These findings may indicate that Fe isotopic signatures in serum may show potential as a biomarker for tau-associated AD. Since the isotopic pattern of the elements in serum can be affected by the food intake, the animals' chow was also analysed (**Table S1**, Supporting Information). As L66 mice exhibit acute neurological phenotype after the tenth month of life, they were supplemented with a protein-enriched chow for animal welfare reasons.

Notably, until the tenth month of life, both L66 and NMRI-mice were fed the same chow. *Post-hoc* analysis demonstrated no difference in the isotopic composition of Fe ($p>0.05$) between the initial and the 10-12th month diet for L66 mice, which was implemented due to animal welfare reasons. However, for Cu and Zn a significant difference in isotopic compositions ($p<0.01$) was observed (**Table S1**, Supporting Information). In principle, the difference (lighter isotopic composition) in the Cu and Zn serum isotopic composition between the L66- and NMRI-WT mice could therefore be (partly) related to the dietary change. Since the L66-mice received a different diet only at the end of the experiment, and the metal content was overall very similar, this is unlikely to dramatically affect the metal contents in brain tissue. The intake between the two different diets varied by some milligrams per kilogram of the chow only (1 mg/kg for Cu, *ca.* +5%; 3 mg/kg for Zn, *ca.* -3%; and 9 mg/kg, *ca.* +5% for Fe). Importantly, for all elements under study, any significant effect of the diet change should not be anticipated. For Fe, there was no difference in isotopic composition between the two diets. For Cu, the observed (not statistically significant) trend towards a lighter isotopic composition in the brain and serum of L66 mice compared to NRMI-WT was the opposite of the dietary change as the 10-12th month chow was enriched in the heavier isotope (^{65}Cu). Additionally, we evaluated the food consumption of the animals based on the body and brain weight at the time of sacrifice (**Table S5** of the Supporting Information). L66 mice had increased normalised brain weights ($p<0.001$), accompanied by decreased body weight ($p<0.001$), compared to the NRMI-WT. This is also confirmed for the 5xFAD model *vs.* BL6-WT ($p<0.05$). This observation may indicate reduced chow consumption in transgenic mice compared to the WTs, which might partially compensate for the effect of the consumption of the different chow in the L66 mice. Nevertheless, specifically, the data on Zn isotopic composition in L66 mice (which were also demonstrated to be not statistically significant) should be considered with care and this can be considered an unavoidable limitation of the current study. The potential effect of the diet must be addressed in further research. For total quantification, significantly increased Fe contents and a tendency towards an increase in the level of Cu and Zn in L66 tau-transgenic mice compared to NMRI-WTs are consistent with previous reports for humans (for review see (14,47)).

The 5xFAD mice and their matching BL6-WT controls were fed with the same chow for the whole duration of the experiment and thus, the potential effect of the diet can be excluded for them. It is noteworthy that except for Cu, the isotopic compositions of Fe and Zn in the chow used to feed the 5xFAD and BL6-WT mice differed significantly (Supporting information, **Table S1**, $p<0.05$) from both chows used to feed the L66 and NMRI-WT mice. Therefore, the differences observed between mouse lines may be, at least partially, attributed to a different nutritional baseline, as well as to a different genetic background. Unfortunately, proper comparison of the two WT lines is not possible due to different age, diet and housing conditions. There was less Cu in brain tissue of the 5xFAD mice compared to BL6-WT. Contrary to that, Zn was accumulated in the brain tissue of 5xFAD mice, which may be attributed to a dysregulated Zn homeostasis between brain and blood (53). Since Aβ aggregation in the brain of these mice starts before 5-6 months of age, this could explain the lower Cu contents in the brain tissues of our 5 months old 5xFAD transgenic mice.

For the 5xFAD mice, a lighter isotopic composition of Zn (Δ^{66}Zn, Δ^{67}Zn and Δ^{68}Zn) was

observed (**Figure 4**). We observed statistical significance (p<0.05) for δ^{67}Zn and δ^{68}Zn only. But as the δ^{66}Zn value is not an independent variable from δ^{67}Zn and δ^{68}Zn due to the mass-dependent nature of the isotope fractionation, the finding for δ^{66}Zn (not significantly different between the groups) may be related to the uncertainty of the measurements. The same may be suggested for the findings for Fe in serum for L66 *vs*. NRMI-WT mice, where only δ^{56}Fe reached the significance level. The difference in the trend for Fe isotopes between 5xFAD and L66 mice may indicate different biochemical pathways involved in changing iron homeostasis under different proteinopathies (54). In the case of tau-pathology in L66 mice, the lighter isotopic composition of Fe may be indicative of its increased turnover in the brain, which is probably not the case for the amyloidogenesis in 5xFAD mice (55). Additionally, the isotopic patterns in blood serum of 5xFAD mice *vs*. BL6-WT were not found to display significant differences for Fe, whilst Zn was slightly enriched in the heavier isotopes in contrast to the corresponding brains. However, in this case the trend is even weaker due to very low levels of Zn in serum of 5xFAD and BL6-WT, leading to higher measurement uncertainty. Importantly, no significant difference in the Cu isotopic composition between transgenic mice and matched WT was found in both AD mouse models.

L66 tau transgenic mice show early-onset and extensive tau pathology in multiple brain regions; these aggregates were reactive with silver and primulin, indicating the formation of stable tau aggregates (24). The tau pathology induces robust motor impairments in line with the symptomatology of FTD patients, such as abnormal gait pattern and dysfunction in motor coordination and motor learning (24). It is therefore not unexpected that metal homeostasis is severely impaired in these mice, also affecting the isotopic compositions of the elements considered. While this is important information for diagnostic considerations, it remains unclear whether it is the result of tau pathology or other disease processes, and whether there may be a causal link.

The 5xFAD mouse model used in the current study is characterized by increased APP expression early in life, modelling familial AD, with pronounced, early amyloid pathology, neuronal loss (33,56) and changes in spine density in the somatosensory and prefrontal cortex by ~6 months of age (57). The age of onset is dependent on the genetic background. For the 5xFAD mouse on BL6/J background used in the current study, brain $A\beta_{42}$ accumulation starts around 2-3 months of age (58). By 4-5 months, the animals exhibit neurological phenotype, including anxiety and freezing-fear behaviour (58,59). The 5xFAD mice develop congophilic amyloid angiopathy (60,61), which also makes them an adequate model for human AD, often containing vascular pathology (62). Additionally, these mice, when kept on a C57BL6/J genetic background, exhibit epileptiform activity, independent of the presence of amyloid plaques, probably related to a high brain APP level *per se* (63). Recently, Bundy *et al*. reported significant alteration of gene expression in 5xFAD female mice compared to matched WT by 4 months of age; many of the altered genes were found to be associated with immune function (50). Thus, by the age of 4-5 months, 5xFAD mice have considerable changes in brain physiology and biochemistry, which may affect metal homeostasis, *e.g*. transition metal turnover and balance, and result in the differences in total levels of the elements and their isotopic composition as observed here.

Since the brain is strongly separated from the periphery by the blood-brain barrier (BBB), the chemical composition of the peripheral fluid like blood serum does not necessarily reflect the composition of the brain compartment (64,65). To test if serum isotopic signatures can be potential biomarkers for changes in brain metal homeostasis in AD model we evaluated linear correlations of the δ-values between brain and blood serum. Mostly not significant correlations were observed, except for δ^{66}Zn in L66 *vs*. NRMI mice, as well as for δ^{65}Cu in L66 mice and for δ^{56}Fe in x5FAD mice but not for the matched WT controls in the case of Cu and Fe. Although the final number of points was rather low to be conclusive, the correlations revealed indicate that the serum isotopic composition is basically independent from that of the brain. This is in line with data for other potential biomarkers in AD (64,66). The entrance of the metal ions and other nutrients to the brain,

as well as the clearance of metabolites and toxins over the BBB, is strictly controlled in the healthy brain (67,68). A wide spectrum of factors is probably involved in clearance and accumulation of the compounds in brain *vs.* blood (68), including transport mechanisms across the BBB, *i.e.* passive diffusion *vs.* active transport, sex, age, circadian rhythm *etc*. Additionally, proteinopathies seem to create specific sinks for toxins such as metals, which may affect the equilibrium between tissues even further. Furthermore, metal ions seem to be able to hijack the corresponding transporters making them prone to accumulate in brain tissue (69), while peripheral levels may remain low. Brain clearance of neurotoxic agents such as, first of all, Aβ and tau, but also other disease-implicated substances, is currently a major research area both for diagnostic and therapeutic advances in dementia research (70). The metals should be addressed more closely in this regard in further studies.

To the best of the authors' knowledge, this is the first study reporting on the Fe isotopic compositions of blood serum and brain tissue in relevant AD models, as well as the first to report on the isotopic composition of Cu, Fe and Zn in tau-transgenic mice. A previous study related to the isotopic composition of Zn as potentially relevant to Alzheimer's disease was published in 2017 by Moynier *et al*. (71). They studied the isotopic signature of Zn in brain tissue, red blood cells and blood serum in 5xFAD compared to WT controls. The sampling was performed at 6, 9 and 12 months. Contrary to our study, the authors reported a heavier Zn isotopic composition in 5xFAD brains compared to that in the WT (significant at $p<0.01$ for 12 months of age). Additionally, a change in the Zn isotopic composition with ageing was also reported, which the authors attributed to the potential increase of free, non-protein bound Zn (71). In a follow-up study, the same group (72) reported isotope ratios for Cu in blood serum and brain tissue of 5xFAD transgenic mice, sampled at the age of 3, 6, 9 and 12 months for blood serum and 9 and 12 months for brain tissue, respectively. Importantly, the authors presented data for both sexes. Similar to our study, no significant difference in the Cu isotopic signature was detected between 5xFAD and WT mice (72). The individual δ-values (Supplementary data file) obtained here for the brain and blood serum were, generally, in line with the previous studies (46). Also, a significantly lighter Cu isotopic composition was observed in serum compared to that of the brain, which is in agreement with previously reported data (46,72).

To conclude, the observed changes in the isotopic pattern of Fe and Zn in the brains and serum may be attributed to different pathological events in transgenic mice. Specific pathological processes in Alzheimer's disease, such as deposition of misfolded protein aggregates of Aβ or hyperphosphorylated tau (54), are clearly accompanied by changes in the brain microenvironment, such as neuroinflammation. All these metals were shown to be modulating both Aβ and tau aggregation at several levels (10,14,73). Their biochemical activity regarding protein folding was rather widely explored in both *in vitro* and *in vivo* studies. For Aβ, those include affecting APP expression (74) and utilisation by α-, β- and γ-secretase (75) and direct binding of Aβ and its oligomers with free metal ions (54,76). Cu, Fe and Zn seem to be involved in tau-pathology by modulating the activity of cyclin-dependent kinase (CDK)5/p25 complex and glycogen synthase kinase-3β (GSK-3) (77-79) or affecting the activity of phosphatase like protein phosphatase 2A (PP2A) (80) and by binding tau *per se*. Metals, first of all, Fe and Zn, binding to Aβ and/or hyperphosphorylated tau might be, at least partially, responsible for the observations of the current study since such binding may induce mass-dependent isotope fractionation (38). However, this notion should be addressed in further research. Another opportunity behind the current observation may be related to the modulation of the metal brain intake. Common features of neurodegenerative disorders are the increased production of reactive oxygen species (81) and the decline of BBB and blood-cerebrospinal fluid barriers (BCSFB) (67,82), both of which may seriously impact the transition metal homeostasis (68). Critically, both animal (83) and human studies (84,85) indicate the vulnerability of the neurovascular unit in AD (86), and both protective and trophic functions of the neural barrier seem to be impaired (82,87). Simultaneously with altered metal-protein interactions due to the complexing capacities of amyloid-β and hyperphosphorylated

tau, the deterioration of the barrier may be one of the reasons for the observed deviation of the isotopic patterns for AD murine models compared to matched WT mice. Reduced BBB integrity may promote excessive exposure of the brain to metal ions such as Fe and Zn leaking from serum proteins (54,88), resulting in a shift in metal binding, releasing more 'free' metal ions or, on the contrary, sequestering them from the normal biochemical turnover. That, in turn, may further exacerbate AD pathology. Metal homeostasis in early *vs*. late dementia, the transport of metals *via* the BBB, and their accumulation profile associated with amyloid *vs*. tau pathologies, should be addressed in future studies, as it may offer both diagnostic and therapeutic opportunities. Other prospects for further research would involve the study of sex and age differences in isotopic signatures of neurodegeneration-associated metals in transgenic mice models and samples of AD patients as well as the isotopic patterns in different brain compartments.

Study strengths and limitations

We consider the use of relevant transgenic mice models of AD and high-precision isotopic analysis as well as inter-laboratory comparisons applied as the strengths of our study. However, this study has certain limitations: different numbers of animals per group were used; for L66 mice a different chow was administered at the end of the of the study due to animal welfare requirements; Fe level and isotopic composition was assessed only in one laboratory, which resulted in a lower number of observations for these parameters; the study was conducted at one fixed age of the animals and with male individuals only, thus, providing no information on potential sex and age effects; finally, Aβ or tau-protein were not assessed in this study.

Experimental Procedures

Mice and tissue

Experiments on animals were carried out in accordance with the European Communities Council Directive (63/2010/EU) with local ethical approval, *i.e.* either a project license issued under the UK Scientific Procedures Act 1986 (PPL 60/4085, for 5xFAD and BL6-WT mice), or in accordance with the German Law for Animal Protection (Tierschutzgesetz; G0068/18, for Line 66 and NMRI-WT mice).

- ***Tau-transgenic mice***

Male homozygous tau-transgenic L66 and NMRI wild-type controls were generated as previously described by Melis *et al*. (24). Two aggregation-promoting mutations, P301S and G335D in the repeat domain, were inserted into the tau cDNA and L66 mice were bred and maintained on an NMRI background. Mice were bred in pressurised isolators and pathogen-free conditions. They were then colony-housed (up to 4 per cage) in Type 2 Macrolon wire lid cages on corn cob bedding in a controlled facility (temperature 20-22°C, 60-65 % humidity, air changes: 17–20 changes per hour). The animals were under a 12-h light/dark cycle and had *ad libitum* access to food and water. In this study, 26 L66 and 14 NMRI-WT mice at 11-12 months of age at the time of sacrifice were used (**Table 1**). Both mouse lines were housed at Charité and received the same chow (V1534-3; metal levels according to the manufacturer, confirmed locally by ICP-MS: 16, 176 and 94 mg/kg for Cu, Fe and Zn, respectively) for the first 10 months. After 10-12 months, when L66 mice developed a considerable tremor, the standard chow had to be substituted with a different chow with higher protein content (V1124-3; metal levels: 17, 185 and 91 mg/kg for Cu, Fe and Zn, respectively) for ethical reasons.

- ***APP/PSEN1 transgenic mice***

Male homozygous 5xFAD-transgenic (5xFAD) and their C57BL6/J wild-type (BL6-WT) littermates were generated as previously described (32). 5xFAD mice were bred and maintained on a C57BL6/J background. Mice were kept in a holding room with a 12-hour light/dark cycle, the temperature was maintained at 23 ± 2ºC and relative humidity was 40–60 %. Mice were allowed *ad libitum* access to food and water (metal levels according to the manufacturer, confirmed locally by ICP-MS: 16, 131 and 87 mg/kg for Cu, Fe and Zn, respectively). Twenty 5xFAD and 20 BL6-WT mice (~5 months of age at the time of sacrifice) were used in this study (**Table 1**). These mice were housed at the University of Aberdeen

and received the same chow during the whole experimentation period.

- ***Perfusion of mice and collection of brain tissue and blood serum***

Mice were injected intraperitoneally with Euthatal as anaesthetic at a dose volume of 10 mL/kg of body weight (5XFAD and BL6-WT) or with ketamine/xylazine (0.2 mL of 100 mg/mL ketamine, 0.2 mL of 20 mg/mL xylazine and 0.6 mL of 0.9 % saline) at a dose volume of 6 mL/kg of body weight (L66 and NMRI-WT). Blood was collected *via* cardiac puncture in lithium-heparin-tubes and the mice were perfused *via* intra-cardiac puncture with heparinised saline solution (50 mg of heparin per litre of 0.9 % saline) for 3 min before harvesting the brains. The brain was separated into hemispheres, transferred into Eppendorf vials and immediately frozen in liquid nitrogen. Blood was centrifuged for 5 min at 2000xg in reaction tubes after standing for 20-30 min. The serum was then transferred into Eppendorf tubes and snap-frozen in liquid nitrogen. Brain and serum samples were kept at -80°C until use. All containers used for sampling were acid and ultra-pure water washed in cleanroom conditions to avoid metal contamination. The body and the brain weights of all mice were taken at the time of sacrifice. Body weight (g), brain weight (mg) and normalised brain weight (brain weight to body weight ratio (mg/g)) are given in **Table S5** (Supporting information).

Analytical methods

The study was conducted at multiple centres. An overview of the study details, including mouse housing facilities and a description of which laboratories involved carried out quantitative determination and isotopic analysis of Fe, Cu and Zn measurements for which sample groups are listed in **Table 1**.

Sample preparation

The analysis of the brain tissue and blood serum was performed at three separate analytical facilities at BAM, Ghent University and University of Aberdeen to ensure data quality. For BAM, all sample preparation steps (except for the digestion step) were carried out in an ISO 6 clean room (PicoTrace); the digestion system and the ICP-MS instruments are in ISO 7 clean rooms. For Ghent University, all sample manipulations were performed in an ISO 4 clean room (PicoTrace). At the University of Aberdeen, all sample preparation steps were carried out in analytical chemistry labs under a laminar flow hood. For quantitative determination of the metal contents, the analytical protocol consisted of the mineralization of the sample (serum and brain tissue) *via* acid digestion. For isotopic analysis, additional sequential chromatographic separation of the target analytes from the matrix is required. The measurements were performed using SF-ICP-MS or Q-ICP-MS and MC-ICP-MS for element content and isotope ratio determination, respectively. Animal chow (0.1 g per replicate) was prepared and analysed analogously with the brain tissue to evaluate the background isotopic composition of the animals.

- ***Digestion procedure***

BAM: In 10-mL quartz vessels, the digestion was accomplished using 3.2 mL and 2.5 mL conc. HNO_3 (67-70 %, purified in-house by two-stage sub-boiling distillation) for brain (whole) and serum samples, respectively. A high-pressure asher system (HPA-S, Anton Paar, Austria) was used for sample digestion. The operating conditions for the HPA-S were: ramping to 300 °C over 30 min and holding at 300 °C for another 90 min and then allowing to cool down. Pressure was set to 100 bar throughout the digestion program. The contents of the digestion vessel were transferred to a 15-mL PFA vessel (Savillex®, USA). The digestion vessel was thoroughly rinsed with 0.28 mol/L HNO_3 and the rinse was transferred to the PFA vessel. The digestion solution was evaporated till dryness at 120 °C. The dried residue was dissolved in 1-2 mL conc. HCl (32-35 %, purified in house by two-stage sub-boiling distillation) and then dried. This process was repeated and the residue was finally redissolved in 8 mol/L HCl + 0.001 % H_2O_2 for the chromatographic separation of Cu, Fe and Zn from the sample matrix.

Ghent University: Ultrapure water (resistivity ≥18.2 MΩ· cm at 25°C) was obtained from a Milli-Q Element water purification system (Merck Millipore, Bedford, MA, USA). Trace metal

analysis grade 14 mol/L HNO_3 and 12 mol/L HCl (PrimarPlus, Fisher Chemicals, Loughborough, Leicestershire, UK) were further purified by sub-boiling distillation in a Savillex DST-4000 acid purification system (Savillex Corporation, Eden Prairie, MN, USA). The purified acids thus obtained were titrated prior use to establish the exact concentration. TraceSELECT® 9.8 mol/L H_2O_2 acquired from Sigma-Aldrich (Overijse, Belgium) was used for sample preparation.

Brain tissue, animal chow, and blood serum samples were digested using a mixture of sub-boiled 14 mol/L HNO_3 and 9.8 mol/L H_2O_2 in Teflon Savillex® beakers at 110 °C for 16 h. 4 mL of HNO_3 and 1 mL of H_2O_2 was used for brain tissue or chow specimens; 2 mL of HNO_3 and 0.5 mL of H_2O_2 were used for blood serum digestion. Subsequently, the sample digests were evaporated to dryness at 90 °C and redissolved in 5 mL of 8 mol/L HCl containing a small amount of H_2O_2 (~0.001 %) to assure occurrence of Cu and Fe in the Cu(II) and Fe (III) oxidation states, respectively, for the chromatographic isolation of the target elements. The samples were used for isotopic analysis only.

University of Aberdeen: Mouse brains were separated into hemispheres prior to digestion. Each hemisphere was 200-400 mg in weight and was digested in 1.5 mL ultrapure concentrated (65 %) nitric acid using a microwave system (Ethos Up, Analytix). Samples were digested in TMF inserts, using a predetermined program with a maximum temperature of 200°C being maintained for 20 minutes and subsequently cooled to < 35°C. Following digestion, samples were diluted to 10 g with ultrapure Milli-Q water. The samples were used for total quantification only.

- ***Target element isolation***

For the determination of isotope ratios at both BAM and Ghent University, Fe, Cu, and Zn were chromatographically separated from the matrix *via* a protocol modified from that developed and reported by Lauwens *et al*. (89) and Van Heghe *et al*. (90) using strong anion exchange resin. Analytical grade AG® MP-1 strong anion exchange resin (100-200 µm dry mesh size, chloride anionic form, Bio-Rad, Temse, Belgium) packed in polypropylene chromatographic columns (Bio-Rad PolyPrep) was used.

The separation procedure is shown in **Table S6** of the Supporting Information. Spectral and non-spectral interferences from concomitant matrix elements were thus virtually eliminated. The purified Fe, Cu and Zn fractions were evaporated till dryness and the residues re-dissolved twice in 14 mol/L HNO_3 to remove residual chlorides. The final residue was re-dissolved in 0.28 mol/L HNO_3 for determination of the total element content and isotope ratios. Quantitative recoveries were obtained for the three elements upon chromatographic separation (~ 100 %), thus ensuring that potential on-column isotope fractionation would not affect the final isotope ratio data.

Determinations by ICP-MS

- ***Total element content***

BAM: The total contents of Cu, Zn and Fe in brain and serum digests were determined *via* external calibration using a single-collector sector field ICP-MS unit (Element 2 / Element XR, Thermo Scientific, Bremen, Germany), operated at medium mass resolution (R ≈ 4000). The instrument was equipped with a jet interface and a sample introduction system consisting of a 200 µL min^{-1} quartz concentric nebulizer and a cyclonic spray chamber. Tuning, mass calibration and determination of mass offsets of the target isotopes were performed before every analytical sequence. In brief, the samples and calibration standards were prepared in 0.28 mol/L HNO_3 and Ge (50 µg/L) was used as an internal standard to correct for matrix effects and instrument instability. The instrument settings and data acquisition parameters are presented in **Table S7** of the Supporting Information. The analytical method was validated using NIST SRM 1598a (Inorganic Constituents in Animal Serum, NIST, USA) and Seronorm® Trace Element Serum level 1 (Sero AS, Norway).

University of Aberdeen: The total contents of Fe, Cu and Zn in brain digests were determined using an Agilent 7900 quadrupole-based ICP-MS instrument using no gas mode for Cu and Zn, and hydrogen gas mode for Fe. During analysis, a 10 µg/L Y and 10 µg/L Rh internal standard solution was continuously introduced into the system. The instrument settings and data acquisition

parameters are presented in **Table S7** of the Supporting Information.

- **Isotope ratios**

Single-element standard stock solutions of Cu, Fe, Zn, Ni and Ga (Inorganic Ventures, the Netherlands) were used for element quantification and mass bias correction. The following isotopic reference materials were used for external mass bias correction: NIST SRM 976 (National Institute of Standards and Technology, Gettysburg, PA, USA) for Cu, IRMM-014 (European Commission, Geel, Belgium) for Fe, and IRMM-3702 (European Commission, Geel, Belgium) for Zn. Single-element standard solutions of Cu, Fe and Zn (Inorganic Ventures, the Netherlands), previously characterized for their isotopic composition (in-house standard solutions), were used for monitoring the quality of the isotope ratio measurements. All standards and samples were properly diluted with 0.28 mol/L HNO_3 for elemental determination and isotope ratio measurement.

Isotope ratio measurements were accomplished using a Neptune multi-collector (MC)-ICP-MS instrument (Thermo Scientific) at both BAM and Ghent University. The instrument settings were tuned daily (Supporting Information, **Table S8**). The measurements were performed at (pseudo) medium mass resolution, in static collection mode and using 10^{11} Ω amplifiers connected to the Faraday collectors. Samples were measured in a sample-standard bracketing approach (SSB).

For SSB, Ghent University used the following isotopic reference materials: NIST SRM 976 for Cu, IRMM-014 for Fe, and IRMM-3702 for Zn. The internal standards used for correction of instrumental mass discrimination were Ni, Ga and Cu for the Fe, Cu and Zn isotope ratio measurements, respectively. Correction for instrumental mass discrimination was performed using a combination of internal correction by means of the revised Russell's law (91) and external correction using the isotopic reference material.

BAM used BAM RS standards as bracketing standard for Cu and Zn. The BAM RS standards were then characterized relative to the isotopic reference materials NIST SRM 976 (Cu, purchased as IRMM-633 from LGC Standards GmbH, Germany) and IRMM-3702 (Zn). The delta values obtained relative to the BAM RS standards were then re-calculated relative to NIST SRM 976 and IRMM-3702, as has been described by Vogl *et al*. (92).

The isotope ratios were expressed in delta notation (δ, per mil, ‰) relative to the respective isotopic reference material and determined using equations (1), (2) and (3) for Cu, Fe and Zn, respectively.

$$\delta^{65}Cu = \left(\frac{\left({}^{65}Cu/{}^{63}Cu\right)_{sample}}{\left({}^{65}Cu/{}^{63}Cu\right)_{standard}} - 1\right) \quad \text{(eqn. 1)}$$

$$\delta^{y}Fe = \left(\frac{\left({}^{y}Fe/{}^{54}Fe\right)_{sample}}{\left({}^{y}Fe/{}^{54}Fe\right)_{standard}} - 1\right) \quad \text{(eqn. 2)}$$

$$\delta^{y}Zn = \left(\frac{\left({}^{y}Zn/{}^{64}Zn\right)_{sample}}{\left({}^{y}Zn/{}^{64}Zn\right)_{standard}} - 1\right) \quad \text{(eqn. 3)}$$

in which *y* is 56 or 57 (for the $^{56/54}$Fe or $^{57/54}$Fe isotope ratios) or 66, 67 or 68 (for the $^{66/64}$Zn, $^{67/64}$Zn or $^{68/64}$ Zn isotope ratios).

Inter-laboratory validation

A rigorous inter-laboratory comparison scheme was executed for quality assurance/quality control (QA/QC). For the total element content, Seronorm® Trace Element Serum level 1 (traceable to NIST SRMs, Sero, Norway) was used as QC samples by BAM and the University of Aberdeen where the validation of the analytical method was performed following the FDA guidelines (93). All recoveries were in agreement with the ± 20% acceptability criteria of the FDA guidelines for method validation (**Table S9 & S10** in the Supporting Information).

BAM and Ghent University were supplied with a QC sample of blood serum, provided by LGC Ltd. (Teddington, London, UK) for isotopic analysis. The QC sample was analysed independently and blindly in accordance to the sample analysis protocol used for the real samples. Acceptable uncertainty ranges were obtained for the Cu, Fe

and Zn isotope ratios (**Table S11 & S12** in the Supporting Information) between BAM and Ghent University.

Statistical analysis

Data analysis was performed using SPSS® Statistics 23 (IBM Corp., Armonk, NY, USA) and Prism 8 (GraphPad Software, San Diego, CA, USA). For each group of mice, median δ-values were calculated and used to evaluate statistical differences between each transgenic model and its respective control group (5xFAD *vs*. BL6-WT and L66 *vs*. NMRI-WT). The outliers were identified using a Grubbs' test (α = 0.05) and excluded from further data evaluation. The normality of the distribution was tested using a Shapiro-Wilk test (α = 0.05) for each group of mice. The difference between the groups based on data obtained in several laboratories (namely, total levels of Cu and Zn in brain, isotopic composition of Cu and Zn, except Zn in blood serum of 5xFAD and BL6-WT mice) was assessed using analysis of covariance (ANCOVA) to exclude the effect of the measurement facility. For the data obtained in a single laboratory only (total Fe in brain, isotopic composition of Fe and isotopic composition of Zn in blood serum of 5xFAD and BL6-WT mice), an unpaired *t*-test or Mann-Whitney rank test was used for normally distributed (parametric) and for non-normally distributed (non-parametric) datasets, respectively. A level of $p<0.05$ was considered as statistically significant.

The correlation between brain and serum isotopic composition were evaluated using Pearson's equation; correlation coefficient (r) and the *p*-value were calculated. Only the subjects for whom the data for both brain tissue and blood serum were available, were included in the correlation analysis.

In case of a statistically significant difference or potential trend in isotopic composition, isotope ratio, the Δ-values were calculated as follows:

$$\Delta^{65}Cu = \left(median[\delta^{65}Cu_{testing\ group}] - median[\delta^{65}Cu_{matched\ control}]\right) \quad \text{(eqn. 4)}$$

$$\Delta^{y}Fe = \left(median[\delta^{y}Fe_{testing\ group}] - median[\delta^{y}Fe_{matched\ control}]\right) \quad \text{(eqn. 5)}$$

$$\Delta^{y}Zn = \left(median[\delta^{y}Zn_{testing\ group}] - median[\delta^{y}Zn_{matched\ control}]\right) \quad \text{(eqn. 6)}$$

in which *y* is 56 or 57 (for the Fe isotope ratios) or 66, 67 or 68 (for the Zn isotope ratios). The use of Δ-values is a conventional approach for the data analysis in isotopic geochemistry (94), which was already applied to biological samples as well (95,96).

Acknowledgements

A.H.E-K thanks Maren Koenig and Dorit Becker for their support in sample preparation. The authors thank Prof. Gernot Riedel, Dr. Silke Frahm and Mandy Magbagbeolu for help with mouse perfusion and harvesting of the brain tissues.

Author contributions

NS, AHE, MCR and EG performed experiments.
NS, AHE, MCR, EG and KS analysed data.
AR, BP, KS, JV, FT and FV conceived the project.
NS, AHE, MCR, KS and JV wrote the paper.
All authors have reviewed and approved the final manuscript.

Funding

This work was carried out in the context of the EMPIR research project 15HLT02 (ReMiND). This project has received funding from the EMPIR programme co-financed by the Participating States and from the European Union's Horizon 2020 research and innovation programme.

Conflict of interest

The authors declare no conflict of interest.

Data availability: Raw data for elemental quantification and isotopic analysis, including statistical processing, are presented in supplementary data file. All remaining data are contained within the article and supplementary tables.

References

1. Gernot, R., Jochen, K., Grazyna, N., Constantin, K., Karima, S., Dilyara, L., Mandy, M., Marta, S., Maciej, Z., Malgorzata, W., Anna, C., Valeria, M., Renato, X. S., Franz, T., Charles, R. H., and Claude, M. W. (2020) Mechanisms of anticholinesterase interference with tau aggregation inhibitor activity in a tau-transgenic mouse model. *Curr Alzheimer Res* **17**, 1-11
2. (2019) 2019 Alzheimer's disease facts and figures. *Alzheimer's & Dementia* **15**, 321-387
3. (2016) 2016 Alzheimer's disease facts and figures. *Alzheimer's & Dementia* **12**, 459-509
4. Lee, J. C., Kim, S. J., Hong, S., and Kim, Y. (2019) Diagnosis of Alzheimer's disease utilizing amyloid and tau as fluid biomarkers. *Exp Mol Med* **51**, 1-10
5. Koss, D. J., Jones, G., Cranston, A., Gardner, H., Kanaan, N. M., and Platt, B. (2016) Soluble pre-fibrillar tau and β-amyloid species emerge in early human Alzheimer's disease and track disease progression and cognitive decline. *Acta Neuropathol* **132**, 875-895
6. Wischik, C. M., Novak, M., Edwards, P. C., Klug, A., Tichelaar, W., and Crowther, R. A. (1988) Structural characterization of the core of the paired helical filament of Alzheimer disease. *Proc Natl Acad Sci U S A* **85**, 4884-4888
7. Wischik, C. M., Edwards, P. C., Lai, R. Y., Roth, M., and Harrington, C. R. (1996) Selective inhibition of Alzheimer disease-like tau aggregation by phenothiazines. *Proc Natl Acad Sci U S A* **93**, 11213-11218
8. Kametani, F., and Hasegawa, M. (2018) Reconsideration of amyloid hypothesis and tau hypothesis in Alzheimer's disease. *Front Neurosci* **12**, 25
9. Michalke, B., and Nischwitz, V. (2010) Review on metal speciation analysis in cerebrospinal fluid-current methods and results: a review. *Anal Chim Acta* **682**, 23-36
10. Roberts, B. R., Ryan, T. M., Bush, A. I., Masters, C. L., and Duce, J. A. (2012) The role of metallobiology and amyloid-beta peptides in Alzheimer's disease. *J Neurochem* **120 Suppl 1**, 149-166
11. Grochowski, C., Blicharska, E., Krukow, P., Jonak, K., Maciejewski, M., Szczepanek, D., Jonak, K., Flieger, J., and Maciejewski, R. (2019) Analysis of trace elements in human brain: its aim, methods, and concentration levels. *Front Chem* **7**, 115
12. Miller, L. M., Wang, Q., Telivala, T. P., Smith, R. J., Lanzirotti, A., and Miklossy, J. (2006) Synchrotron-based infrared and X-ray imaging shows focalized accumulation of Cu and Zn co-localized with beta-amyloid deposits in Alzheimer's disease. *J Struct Biol* **155**, 30-37
13. Bush, A. I. (2013) The metal theory of Alzheimer's disease. *J Alzheimers Dis* **33 Suppl 1**, S277-281
14. Kim, A. C., Lim, S., and Kim, Y. K. (2018) Metal ion effects on abeta and tau aggregation. *Int J Mol Sci* **19**
15. Ahmadi, S., Zhu, S., Sharma, R., Wilson, D. J., and Kraatz, H. B. (2019) Interaction of metal ions with tau protein. The case for a metal-mediated tau aggregation. *J Inorg Biochem* **194**, 44-51
16. Killin, L. O. J., Starr, J. M., Shiue, I. J., and Russ, T. C. (2016) Environmental risk factors for dementia: a systematic review. *BMC Geriatr* **16**, 175

17. Cicero, C. E., Mostile, G., Vasta, R., Rapisarda, V., Signorelli, S. S., Ferrante, M., Zappia, M., and Nicoletti, A. (2017) Metals and neurodegenerative diseases. A systematic review. *Environ Res* **159**, 82-94
18. Bonda, D. J., Lee, H.-g., Blair, J. A., Zhu, X., Perry, G., and Smith, M. A. (2011) Role of metal dyshomeostasis in Alzheimer's disease. *Metallomics* **3**, 267-270
19. Savelieff, M. G., Lee, S., Liu, Y., and Lim, M. H. (2013) Untangling Amyloid-β, Tau, and Metals in Alzheimer's Disease. *ACS Chem Biol* **8**, 856-865
20. Adlard, P. A., and Bush, A. I. (2018) Metals and Alzheimer's disease: how far have we come in the clinic? *J Alzheimers Dis* **62**, 1369-1379
21. Götz, J., Chen, F., van Dorpe, J., and Nitsch, R. M. (2001) Formation of neurofibrillary tangles in P301L tau transgenic mice induced by Aβ42 fibrils. *Science* **293**, 1491
22. Yanamandra, K., Jiang, H., Mahan, T. E., Maloney, S. E., Wozniak, D. F., Diamond, M. I., and Holtzman, D. M. (2015) Anti-tau antibody reduces insoluble tau and decreases brain atrophy. *Ann Clin Transl Neurol* **2**, 278-288
23. Lewis, J., McGowan, E., Rockwood, J., Melrose, H., Nacharaju, P., Van Slegtenhorst, M., Gwinn-Hardy, K., Murphy, M. P., Baker, M., Yu, X., Duff, K., Hardy, J., Corral, A., Lin, W.-L., Yen, S.-H., Dickson, D. W., Davies, P., and Hutton, M. (2000) Neurofibrillary tangles, amyotrophy and progressive motor disturbance in mice expressing mutant (P301L) tau protein. *Nat Genet* **25**, 402-405
24. Melis, V., Zabke, C., Stamer, K., Magbagbeolu, M., Schwab, K., Marschall, P., Veh, R. W., Bachmann, S., Deiana, S., Moreau, P. H., Davidson, K., Harrington, K. A., Rickard, J. E., Horsley, D., Garman, R., Mazurkiewicz, M., Niewiadomska, G., Wischik, C. M., Harrington, C. R., Riedel, G., and Theuring, F. (2015) Different pathways of molecular pathophysiology underlie cognitive and motor tauopathy phenotypes in transgenic models for Alzheimer's disease and frontotemporal lobar degeneration. *Cell Mol Life Sci* **72**, 2199-2222
25. Goedert, M., Crowther, R. A., and Spillantini, M. G. (1998) Tau mutations cause frontotemporal dementias. *Neuron* **21**, 955-958
26. Hutton, M., Lendon, C. L., Rizzu, P., Baker, M., Froelich, S., Houlden, H., Pickering-Brown, S., Chakraverty, S., Isaacs, A., Grover, A., Hackett, J., Adamson, J., Lincoln, S., Dickson, D., Davies, P., Petersen, R. C., Stevens, M., de Graaff, E., Wauters, E., van Baren, J., Hillebrand, M., Joosse, M., Kwon, J. M., Nowotny, P., Che, L. K., Norton, J., Morris, J. C., Reed, L. A., Trojanowski, J., Basun, H., Lannfelt, L., Neystat, M., Fahn, S., Dark, F., Tannenberg, T., Dodd, P. R., Hayward, N., Kwok, J. B. J., Schofield, P. R., Andreadis, A., Snowden, J., Craufurd, D., Neary, D., Owen, F., Oostra, B. A., Hardy, J., Goate, A., van Swieten, J., Mann, D., Lynch, T., and Heutink, P. (1998) Association of missense and 5′-splice-site mutations in tau with the inherited dementia FTDP-17. *Nature* **393**, 702-705
27. Spillantini, M. G., Crowther, R. A., Kamphorst, W., Heutink, P., and van Swieten, J. C. (1998) Tau pathology in two dutch families with mutations in the microtubule-binding region of tau. *Am J Pathol* **153**, 1359-1363
28. Cranston, A. L., Wysocka, A., Steczkowska, M., Zadrożny, M., Palasz, E., Harrington, C. R., Theuring, F., Wischik, C. M., Riedel, G., and Niewiadomska, G. (2020) Cholinergic and inflammatory phenotypes in transgenic tau mouse models of Alzheimer's disease and frontotemporal lobar degeneration. *Brain Communications*

29. Quon, D., Wang, Y., Catalano, R., Scardina, J. M., Murakami, K., and Cordell, B. (1991) Formation of β-amyloid protein deposits in brains of transgenic mice. *Nature* **352**, 239-241
30. Fukuchi, K., Ho, L., Younkin, S. G., Kunkel, D. D., Ogburn, C. E., LeBoeuf, R. C., Furlong, C. E., Deeb, S. S., Nochlin, D., Wegiel, J., Wisniewski, H. M., and Martin, G. M. (1996) High levels of circulating beta-amyloid peptide do not cause cerebral beta-amyloidosis in transgenic mice. *Am J Pathol* **149**, 219-227
31. Esquerda-Canals, G., Montoliu-Gaya, L., Güell-Bosch, J., and Villegas, S. (2017) Mouse models of Alzheimer's disease. *J Alzheimers Dis* **57**, 1171-1183
32. Oakley, H., Cole, S. L., Logan, S., Maus, E., Shao, P., Craft, J., Guillozet-Bongaarts, A., Ohno, M., Disterhoft, J., Van Eldik, L., Berry, R., and Vassar, R. (2006) Intraneuronal beta-amyloid aggregates, neurodegeneration, and neuron loss in transgenic mice with five familial Alzheimer's disease mutations: potential factors in amyloid plaque formation. *J Neurosci* **26**, 10129-10140
33. Jawhar, S., Trawicka, A., Jenneckens, C., Bayer, T. A., and Wirths, O. (2012) Motor deficits, neuron loss, and reduced anxiety coinciding with axonal degeneration and intraneuronal Abeta aggregation in the 5XFAD mouse model of Alzheimer's disease. *Neurobiol Aging* **33**, 196 e129-140
34. Solovyev, N., Vanhaecke, F., and Michalke, B. (2019) Selenium and iodine in diabetes mellitus with a focus on the interplay and speciation of the elements. *J Trace Elem Med Biol* **56**, 69-80
35. Vanhaecke, F., and Degryse, P. (eds). (2012) *Isotopic Analysis – Fundamentals and Applications Using ICP-MS*, Wiley-VCH, Weinheim
36. Vanhaecke, F., Balcaen, L., and Malinovsky, D. (2009) Use of single-collector and multi-collector ICP-mass spectrometry for isotopic analysis. *J Anal Atom Spectrom* **24**, 863-886
37. Albarede, F., Telouk, P., Balter, V., Bondanese, V. P., Albalat, E., Oger, P., Bonaventura, P., Miossec, P., and Fujii, T. (2016) Medical applications of Cu, Zn, and S isotope effects. *Metallomics* **8**, 1056-1070
38. Costas-Rodríguez, M., Delanghe, J., and Vanhaecke, F. (2016) High-precision isotopic analysis of essential mineral elements in biomedicine: natural isotope ratio variations as potential diagnostic and/or prognostic markers. *TrAC-Trend Anal Chem* **76**, 182-193
39. Costas-Rodriguez, M., Anoshkina, Y., Lauwens, S., Van Vlierberghe, H., Delanghe, J., and Vanhaecke, F. (2015) Isotopic analysis of Cu in blood serum by multi-collector ICP-mass spectrometry: a new approach for the diagnosis and prognosis of liver cirrhosis? *Metallomics* **7**, 491-498
40. Balter, V., Nogueira da Costa, A., Bondanese, V. P., Jaouen, K., Lamboux, A., Sangrajrang, S., Vincent, N., Fourel, F., Telouk, P., Gigou, M., Lecuyer, C., Srivatanakul, P., Brechot, C., Albarede, F., and Hainaut, P. (2015) Natural variations of copper and sulfur stable isotopes in blood of hepatocellular carcinoma patients. *Proc Natl Acad Sci U S A* **112**, 982-985
41. Hastuti, A. A. M. B., Costas-Rodríguez, M., Matsunaga, A., Ichinose, T., Hagiwara, S., Shimura, M., and Vanhaecke, F. (2020) Cu and Zn isotope ratio variations in plasma for survival prediction in hematological malignancy cases. *Sci Rep* **10**, 16389

42. Hotz, K., Augsburger, H., and Walczyk, T. (2011) Isotopic signatures of iron in body tissues as a potential biomarker for iron metabolism. *J Anal Atom Spectrom* **26**, 1347-1353
43. Anoshkina, Y., Costas-Rodriguez, M., Speeckaert, M., Van Biesen, W., Delanghe, J., and Vanhaecke, F. (2017) Iron isotopic composition of blood serum in anemia of chronic kidney disease. *Metallomics* **9**, 517-524
44. Larner, F., Woodley, L. N., Shousha, S., Moyes, A., Humphreys-Williams, E., Strekopytov, S., Halliday, A. N., Rehkämper, M., and Coombes, R. C. (2015) Zinc isotopic compositions of breast cancer tissue. *Metallomics* **7**, 112-117
45. Schilling, K., Larner, F., Saad, A., Roberts, R., Kocher, H. M., Blyuss, O., Halliday, A. N., and Crnogorac-Jurcevic, T. (2020) Urine metallomics signature as an indicator of pancreatic cancer. *Metallomics* **12**, 752-757
46. Balter, V., Lamboux, A., Zazzo, A., Telouk, P., Leverrier, Y., Marvel, J., Moloney, A. P., Monahan, F. J., Schmidt, O., and Albarede, F. (2013) Contrasting Cu, Fe, and Zn isotopic patterns in organs and body fluids of mice and sheep, with emphasis on cellular fractionation. *Metallomics* **5**, 1470-1482
47. Mahan, B., Moynier, F., Jørgensen, A. L., Habekost, M., and Siebert, J. (2018) Examining the homeostatic distribution of metals and Zn isotopes in Göttingen minipigs. *Metallomics* **10**, 1264-1281
48. Costas-Rodríguez, M., Van Campenhout, S., Hastuti, A. A. M. B., Devisscher, L., Van Vlierberghe, H., and Vanhaecke, F. (2019) Body distribution of stable copper isotopes during the progression of cholestatic liver disease induced by common bile duct ligation in mice. *Metallomics* **11**, 1093-1103
49. Ferretti, M. T., Iulita, M. F., Cavedo, E., Chiesa, P. A., Schumacher Dimech, A., Santuccione Chadha, A., Baracchi, F., Girouard, H., Misoch, S., Giacobini, E., Depypere, H., Hampel, H., for the Women's Brain, P., and the Alzheimer Precision Medicine, I. (2018) Sex differences in Alzheimer disease — the gateway to precision medicine. *Nat Rev Neurol* **14**, 457-469
50. Bundy, J. L., Vied, C., Badger, C., and Nowakowski, R. S. (2019) Sex-biased hippocampal pathology in the 5XFAD mouse model of Alzheimer's disease: A multi-omic analysis. *J Comp Neurol* **527**, 462-475
51. Maynard, C. J., Cappai, R., Volitakis, I., Cherny, R. A., White, A. R., Beyreuther, K., Masters, C. L., Bush, A. I., and Li, Q.-X. (2002) Overexpression of Alzheimer's Disease amyloid-β opposes the age-dependent elevations of brain copper and iron. *J Biol Chem* **277**, 44670-44676
52. Maynard, C. J., Cappai, R., Volitakis, I., Cherny, R. A., Masters, C. L., Li, Q.-X., and Bush, A. I. (2006) Gender and genetic background effects on brain metal levels in APP transgenic and normal mice: Implications for Alzheimer β-amyloid pathology. *J Inorg Biochem* **100**, 952-962
53. Baum, L., Chan, I. H., Cheung, S. K., Goggins, W. B., Mok, V., Lam, L., Leung, V., Hui, E., Ng, C., Woo, J., Chiu, H. F., Zee, B. C., Cheng, W., Chan, M. H., Szeto, S., Lui, V., Tsoh, J., Bush, A. I., Lam, C. W., and Kwok, T. (2010) Serum zinc is decreased in Alzheimer's disease and serum arsenic correlates positively with cognitive ability. *Biometals* **23**, 173-179

54. Linert, W., and Kozlowski, H. (2012) *Metal Ions in Neurological Systems*, Springer-Verlag Wien, Vienna
55. Kozlowski, H., Luczkowski, M., Remelli, M., and Valensin, D. (2012) Copper, zinc and iron in neurodegenerative diseases (Alzheimer's, Parkinson's and prion diseases). *Coordi Chem Rev* **256**, 2129-2141
56. Buskila, Y., Crowe, S. E., and Ellis-Davies, G. C. R. (2013) Synaptic deficits in layer 5 neurons precede overt structural decay in 5xFAD mice. *Neuroscience* **254**, 152-159
57. Crowe, S. E., and Ellis-Davies, G. C. R. (2014) Spine pruning in 5xFAD mice starts on basal dendrites of layer 5 pyramidal neurons. *Brain Struct Funct* **219**, 571-580
58. Guo, Q., Li, H., Cole, A. L., Hur, J.-Y., Li, Y., and Zheng, H. (2013) Modeling Alzheimer's disease in mouse without mutant protein overexpression: Cooperative and independent effects of Aβ and tau. *PLOS ONE* **8**, e80706
59. Guo, Q., Zheng, H., and Justice, N. J. (2012) Central CRF system perturbation in an Alzheimer's disease knockin mouse model. *Neurobiol Aging* **33**, 2678-2691
60. Guzmán, E. A., Bouter, Y., Richard, B. C., Lannfelt, L., Ingelsson, M., Paetau, A., Verkkoniemi-Ahola, A., Wirths, O., and Bayer, T. A. (2014) Abundance of $A\beta_5$-x like immunoreactivity in transgenic 5XFAD, APP/PS1KI and 3xTG mice, sporadic and familial Alzheimer's disease. *Mol Neurodegener* **9**, 13-13
61. Giannoni, P., Arango-Lievano, M., Neves, I. D., Rousset, M.-C., Baranger, K., Rivera, S., Jeanneteau, F., Claeysen, S., and Marchi, N. (2016) Cerebrovascular pathology during the progression of experimental Alzheimer's disease. *Neurobiol Dis* **88**, 107-117
62. Attems, J., and Jellinger, K. A. (2014) The overlap between vascular disease and Alzheimer's disease - lessons from pathology. *BMC Med* **12**, 206
63. Born, H. A., Kim, J.-Y., Savjani, R. R., Das, P., Dabaghian, Y. A., Guo, Q., Yoo, J. W., Schuler, D. R., Cirrito, J. R., Zheng, H., Golde, T. E., Noebels, J. L., and Jankowsky, J. L. (2014) Genetic suppression of transgenic APP rescues Hypersynchronous network activity in a mouse model of Alzeimer's disease. *J Neurosci* **34**, 3826-3840
64. Plucińska, K., Dekeryte, R., Koss, D., Shearer, K., Mody, N., Whitfield, P. D., Doherty, M. K., Mingarelli, M., Welch, A., Riedel, G., Delibegovic, M., and Platt, B. (2016) Neuronal human BACE1 knockin induces systemic diabetes in mice. *Diabetologia* **59**, 1513-1523
65. Michalke, B., Willkommen, D., Drobyshev, E., and Solovyev, N. (2018) The importance of speciation analysis in neurodegeneration research. *TrAC-Trend Anal Chem* **104**, 160-170
66. Huo, Z., Yu, L., Yang, J., Zhu, Y., Bennett, D. A., and Zhao, J. (2020) Brain and blood metabolome for Alzheimer's dementia: findings from a targeted metabolomics analysis. *Neurobiol Aging* **86**, 123-133
67. Erickson, M. A., and Banks, W. A. (2013) Blood–brain barrier dysfunction as a cause and consequence of Alzheimer's disease. *J Cerebr Blood F Met* **33**, 1500-1513
68. Campos-Bedolla, P., Walter, F. R., Veszelka, S., and Deli, M. A. (2014) Role of the blood–brain barrier in the nutrition of the central nervous system. *Arch Med Res* **45**, 610-638
69. Bal, W., Sokołowska, M., Kurowska, E., and Faller, P. (2013) Binding of transition metal ions to albumin: Sites, affinities and rates. *BBA – Gen Subjects* **1830**, 5444-5455
70. Deane, R., Bell, R. D., Sagare, A., and Zlokovic, B. V. (2009) Clearance of amyloid-β peptide across the blood-brain barrier: implication for therapies in Alzheimers disease. *CNS & Neurological Disorders - Drug Targets* **8**, 16-30

71. Moynier, F., Foriel, J., Shaw, A. S., and Le Borgne, M. (2017) Distribution of Zn isotopes during Alzheimer's disease. *Geochemical Perspectives Letters* **3**, 142-150
72. Moynier, F., Creech, J., Dallas, J., and Le Borgne, M. (2019) Serum and brain natural copper stable isotopes in a mouse model of Alzheimer's disease. *Sci Rep* **9**, 11894
73. Rao, S. S., and Adlard, P. A. (2018) Untangling tau and iron: Exploring the interaction between iron and tau in neurodegeneration. *Frontiers in Molecular Neuroscience* **11**
74. Rogers, J. T., Randall, J. D., Cahill, C. M., Eder, P. S., Huang, X., Gunshin, H., Leiter, L., McPhee, J., Sarang, S. S., Utsuki, T., Greig, N. H., Lahiri, D. K., Tanzi, R. E., Bush, A. I., Giordano, T., and Gullans, S. R. (2002) An Iron-responsive element type ii in the 5′ -untranslated region of the Alzheimer's amyloid precursor protein transcript. *J Biol Chem* **277**, 45518-45528
75. Gerber, H., Wu, F., Dimitrov, M., Garcia Osuna, G. M., and Fraering, P. C. (2017) Zinc and copper differentially modulate amyloid precursor protein processing by γ-secretase and amyloid-β peptide production. *J Biol Chem* **292**, 3751-3767
76. Boopathi, S., and Kolandaivel, P. (2016) Fe2+ binding on amyloid β-peptide promotes aggregation. *Proteins* **84**, 1257-1274
77. Kitazawa, M., Cheng, D., and LaFerla, F. M. (2009) Chronic copper exposure exacerbates both amyloid and tau pathology and selectively dysregulates cdk5 in a mouse model of AD. *J Neurochem* **108**, 1550-1560
78. Crouch, P. J., Hung, L. W., Adlard, P. A., Cortes, M., Lal, V., Filiz, G., Perez, K. A., Nurjono, M., Caragounis, A., Du, T., Laughton, K., Volitakis, I., Bush, A. I., Li, Q.-X., Masters, C. L., Cappai, R., Cherny, R. A., Donnelly, P. S., White, A. R., and Barnham, K. J. (2009) Increasing Cu bioavailability inhibits Aβ oligomers and tau phosphorylation. *Proc Natl Acad Sci U S A* **106**, 381-386
79. Guo, C., Wang, P., Zhong, M.-L., Wang, T., Huang, X.-S., Li, J.-Y., and Wang, Z.-Y. (2013) Deferoxamine inhibits iron induced hippocampal tau phosphorylation in the Alzheimer transgenic mouse brain. *Neurochem Int* **62**, 165-172
80. Xiong, Y., Luo, D.-J., Wang, X.-L., Qiu, M., Yang, Y., Yan, X., Wang, J.-Z., Ye, Q.-F., and Liu, R. (2015) Zinc binds to and directly inhibits protein phosphatase 2A in vitro. *Neurosci Bull* **31**, 331-337
81. Loef, M., Schrauzer, G. N., and Walach, H. (2011) Selenium and Alzheimer's disease: a systematic review. *J Alzheimers Dis* **26**, 81-104
82. Balusu, S., Brkic, M., Libert, C., and Vandenbroucke, R. (2016) The choroid plexus-cerebrospinal fluid interface in Alzheimer's disease: more than just a barrier. *Neural Regeneration Research* **11**, 534-537
83. Sengillo, J. D., Winkler, E. A., Walker, C. T., Sullivan, J. S., Johnson, M., and Zlokovic, B. V. (2013) Deficiency in mural vascular cells coincides with blood-brain barrier disruption in Alzheimer's disease. *Brain Pathol* **23**, 303-310
84. Halliday, M. R., Rege, S. V., Ma, Q., Zhao, Z., Miller, C. A., Winkler, E. A., and Zlokovic, B. V. (2016) Accelerated pericyte degeneration and blood–brain barrier breakdown in apolipoprotein E4 carriers with Alzheimer's disease. *J Cerebr Blood F Met* **36**, 216-227
85. Skillbäck, T., Delsing, L., Synnergren, J., Mattsson, N., Janelidze, S., Nägga, K., Kilander, L., Hicks, R., Wimo, A., Winblad, B., Hansson, O., Blennow, K., Eriksdotter, M., and

Zetterberg, H. (2017) CSF/serum albumin ratio in dementias: a cross-sectional study on 1861 patients. *Neurobiol Aging* **59**, 1-9
86. Muoio, V., Persson, P. B., and Sendeski, M. M. (2014) The neurovascular unit – concept review. *Acta Physiol* **210**, 790-798
87. Zenaro, E., Piacentino, G., and Constantin, G. (2017) The blood-brain barrier in Alzheimer's disease. *Neurobiol Dis* **107**, 41-56
88. Choi, T. S., Lee, H. J., Han, J. Y., Lim, M. H., and Kim, H. I. (2017) Molecular insights into human serum albumin as a receptor of amyloid-β in the extracellular region. *J Amer Chem Soc* **139**, 15437-15445
89. Lauwens, S., Costas-Rodriguez, M., Van Vlierberghe, H., and Vanhaecke, F. (2016) Cu isotopic signature in blood serum of liver transplant patients: a follow-up study. *Sci Rep* **6**, 30683
90. Van Heghe, L., Engström, E., Rodushkin, I., Cloquet, C., and Vanhaecke, F. (2012) Isotopic analysis of the metabolically relevant transition metals Cu, Fe and Zn in human blood from vegetarians and omnivores using multi-collector ICP-mass spectrometry. *J Anal Atom Spectrom* **27**, 1327-1334
91. Baxter, D. C., Rodushkin, I., Engström, E., and Malinovsky, D. (2006) Revised exponential model for mass bias correction using an internal standard for isotope abundance ratio measurements by multi-collector inductively coupled plasma mass spectrometry. *J Anal Atom Spectrom* **21**, 427-430
92. Vogl, J., and Pritzkow, W. (2010) Isotope reference materials for present and future isotope research. *Journal of Analytical Atomic Spectrometry* **25**, 923-932
93. Gray, P. J., Mindak, W. R., and Cheng, J. (2015) Inductively coupled plasma-mass spectrometric determination of arsenic, cadmium, chromium, lead, mercury, and other elements in food using microwave assisted digestion. *U.S. Food and Drug Administration*
94. Coplen, T. B. (2011) Guidelines and recommended terms for expression of stable-isotope-ratio and gas-ratio measurement results. *Rapid Communications in Mass Spectrometry* **25**, 2538-2560
95. Geilert, S., Vogl, J., Rosner, M., and Eichert, T. (2019) Boron isotope variability related to boron speciation (change during uptake and transport) in bell pepper plants and SI traceable n(11B)/n(10B) ratios for plant reference materials. *Rapid Communications in Mass Spectrometry* **33**, 1137-1147
96. Sullivan, K., Moore, R. E. T., Rehkämper, M., Layton-Matthews, D., Leybourne, M. I., Puxty, J., and Kyser, T. K. (2020) Postprandial zinc stable isotope response in human blood serum. *Metallomics*, 10.1039/D1030MT00122H

Table 1.

Mouse groups and cohort sizes (n) used to measure total Fe, Cu and Zn contents in brain tissue as well as their isotopic composition in brain and serum samples. Details for mouse housing facilities as well as for facilities conducting MS measurements are indicated. IR: isotope ratio, * – Reduced mouse number included in the analyses due to failed sampling. **: IR analysis of mouse chow was conducted at Ghent University. All animals were males.

Housing facility	Mouse line	Tissue	Metal	n	Analytical research facility
Charité - Berlin	L66**	Brain	Total Fe	13	University of Aberdeen (n = 13)
			Total Cu	26	BAM (n = 13) and University of Aberdeen (n = 13)
			Total Zn	26	BAM (n = 13) and University of Aberdeen (n = 13)
			IR Fe	13	Ghent University (n = 13)
			IR Cu	26	BAM (n = 13), Ghent University (n = 13)
			IR Zn	26	BAM (n = 13), Ghent University (n = 13)
		Serum	IR Fe	13	Ghent University (n = 13)
			IR Cu	24	BAM (n = 11), Ghent University (n = 13)
			IR Zn	24	BAM (n = 11), Ghent University (n = 13)
Charité - Berlin	NMRI-WT**	Brain	Total Fe	5	University of Aberdeen (n = 5)
			Total Cu	11	BAM (n = 6), University of Aberdeen (n = 5)
			Total Zn	11	BAM (n = 6), University of Aberdeen (n = 5)
			IR Fe	5	Ghent University (n = 5)
			IR Cu	11	BAM (n = 6), Ghent University (n = 5)
			IR Zn	11	BAM (n = 6), Ghent University (n = 5)
		Serum	IR Fe	5	Ghent University (n = 5)
			IR Cu	9	BAM (n = 4), Ghent University (n = 5)
			IR Zn	9	BAM (n = 4), Ghent University (n = 5)
University of Aberdeen	5xFAD**	Brain	Total Fe	8	University of Aberdeen (n = 8)
			Total Cu	18	BAM (n = 10), University of Aberdeen (n = 8)
			Total Zn	18	BAM (n = 10), University of Aberdeen (n = 8)
			IR Fe	10	Ghent University (n = 10)
			IR Cu	20	BAM (n = 10), Ghent University (n = 10)
			IR Zn	20	BAM (n = 10), Ghent University (n = 10)
		Serum	IR Fe	9*	Ghent University (n = 9)
			IR Cu	14*	BAM (n = 5), Ghent University (n = 9)
			IR Zn	9*	Ghent University (n = 9)
University of Aberdeen	BL6-WT**	Brain	Total Fe	9	University of Aberdeen (n = 9)
			Total Cu	19	BAM (n = 10), University of Aberdeen (n = 9)
			Total Zn	19	BAM (n = 10), University of Aberdeen (n = 9)
			IR Fe	10	Ghent University (n = 10)
			IR Cu	20	BAM (n = 10), Ghent University (n = 10)
			IR Zn	20	BAM (n = 10), Ghent University (n = 10)
		Serum	IR Fe	8*	Ghent University (n = 8)
			IR Cu	14*	BAM (n = 6), Ghent University (n = 8)
			IR Zn	8*	Ghent University (n = 8)

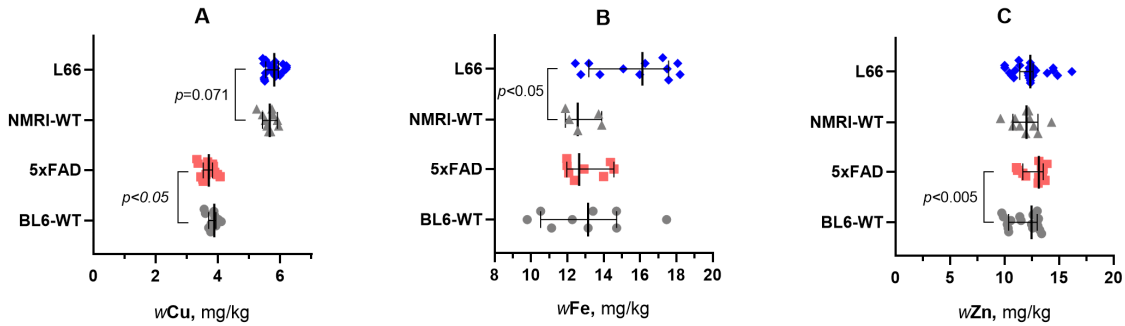

Figure 1. Cu (A), Fe (B) and Zn (C) contents (in mg per kg of wet tissue) in brain tissue of L66 and 5xFAD mice relative to matched WT-controls. Values are presented as dot scatter plots showing the median with error bars indicating the 95% CI. Total element contents were measured by ICP-MS. Statistical analysis was conducted using ANCOVA (**A** and **C**) and *t*-tests (**B**). All animals were males; the age of the animals was 11-12 months and 5-6 months for L66/NMRI-WT and 5xFAD/BL6-WT, respectively. Detailed data are presented in **Table S2** (Supporting information). The numbers of animals analysed at the different research facilities are indicated in **Table 1**.

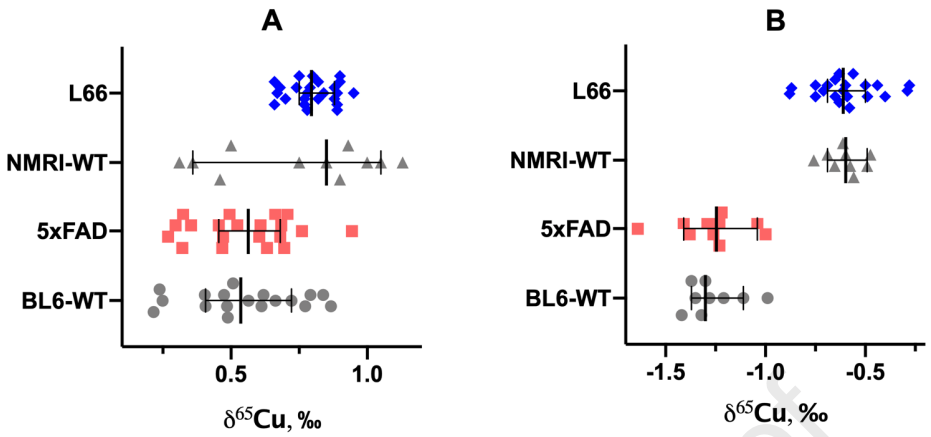

Figure 2. Isotopic signatures of copper (δ^{65}Cu) in brain (A) and blood serum (B) of L66 *vs.* NMRI-WT and 5xFAD *vs.* BL6-WT mice. Values are presented as dot scatter plots showing the median with error bars indicating the 95% CI. Isotope ratios were measured by MC-ICP-MS. Statistical analysis was conducted using ANCOVA. Detailed data are presented in **Tables S3** & **S4** (Supporting information). All animals were males; was 11-12 months and 5-6 months L66/NMRI-WT and 5xFAD/BL6-WT, respectively. The numbers of animals analysed at the different research facilities are indicated in **Table 1**.

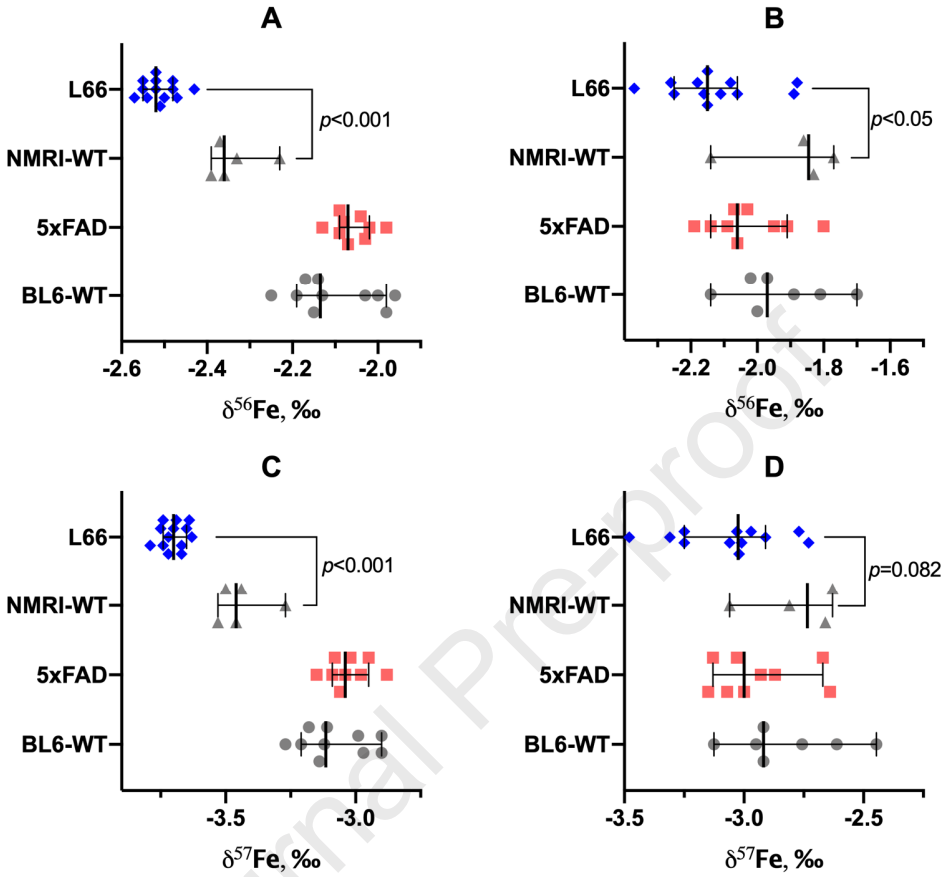

Figure 3. Isotopic signatures of iron (δ^{56}Fe – A and B; δ^{57}Fe – C and D) in brain (A and C) and blood serum (B and D) of L66 *vs.* NMRI-WT and 5xFAD *vs.* BL6-WT mice. Values are presented as dot scatter plots showing the median with error bars indicating the 95% CI. Isotope ratios were measured by MC-ICP-MS. Statistical analysis was conducted using a Mann-Whitney rank test. Detailed data are presented in **Tables S3** & **S4** (Supporting information). All animals were males; was 11-12 months and 5-6 months for L66/NMRI-WT and 5xFAD/BL6-WT, respectively. The numbers of animals analysed at the different research facilities are indicated in **Table 1**.

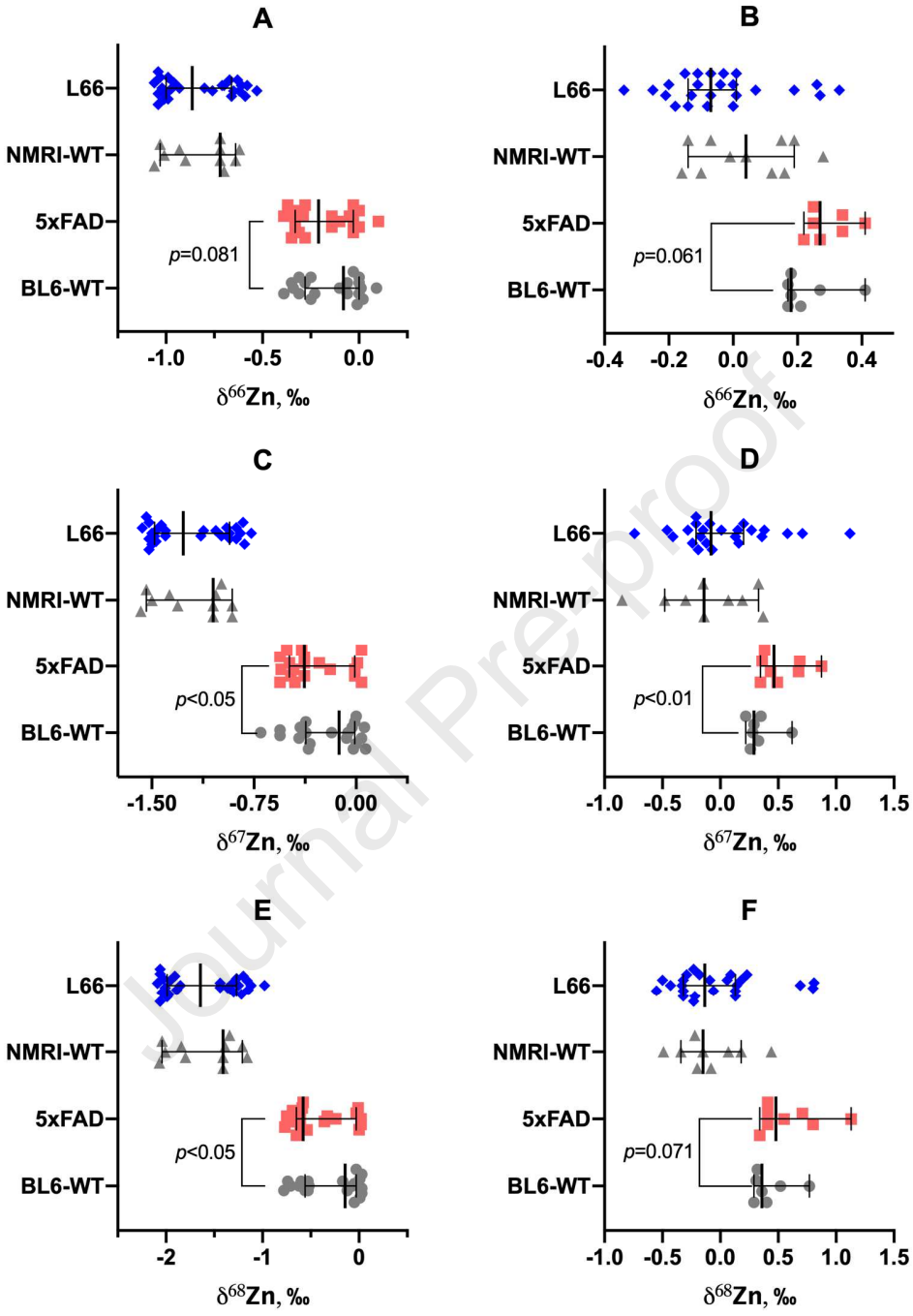

Figure 4. Isotopic signatures of zinc (δ^{66}Zn – A and B; δ^{67}Zn – C and D; δ^{68}Zn – E and F) in brain (A, C and E) and blood serum (B, D and F) of L66 *vs.* NMRI-WT and 5xFAD *vs.* BL6-WT mice. Values are presented as dot scatter plots showing the median with error bars indicating the 95% CI. Isotope ratios were measured by MC-ICP-MS. Statistical analysis was conducted using ACOVA and a Mann-Whitney rank test (only for 5xFAD and BL6-WT in B, D and F). Detailed data are presented in **Tables S3** & **S4** (Supporting information). All animals were males; was 11-12 months and 5-6 months L66/NMRI-WT and 5xFAD/BL6-WT, respectively. The numbers of the animals analysed at the different research facilities are indicated in **Table 1**.

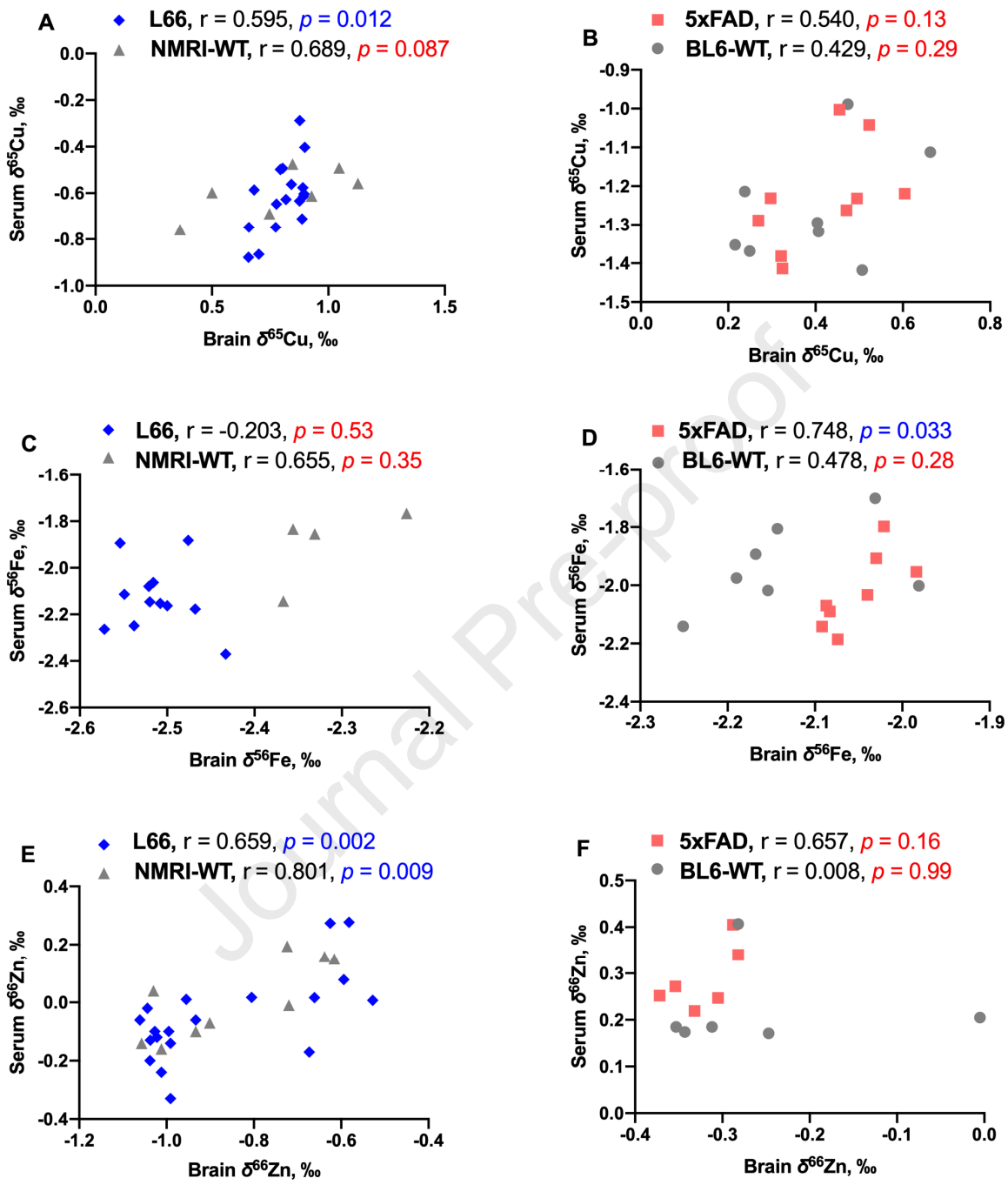

Figure 5. Pearson's correlations of δ^{65}Cu (A and B), δ^{56}Fe (C and D) and δ^{66}Zn (E and F) values between brain and blood serum for L66 (blue diamonds) and NMRI-WT controls (grey triangles) – A, C and E; for 5xFAD mice (red square) and matched BL6-WT (grey circles) – B, D and F. Linear regressions were calculated by Pearson's correlation and correlation coefficient r between pairs is given in the figure. Statistically significant correlations ($p < 0.05$) are indicated in blue font, while values that are not statistically significant are marked in red. All animals were males; the age of L66 and NMRI-WT mice was 11-12 months; the age of 5xFAD and BL6-WT animals was 5-6 months. The numbers of animals analysed at the different research facilities are indicated in **Table 1**.